Journal of Porous Media, 24(1):81–100 (2021)

HEAT AND MASS TRANSFER ON UNSTEADY MHD FLOW THROUGH AN INFINITE OSCILLATING VERTICAL POROUS SURFACE

M. Veera Krishna,[1,] M. Gangadhar Reddy,[2] & A.J. Chamkha[3,4]*

[1]*Department of Mathematics, Rayalaseema University, Kurnool, Andhra Pradesh 518007, India*

[2]*Department of Science and Humanities, Sri Venkateswara Institute of Science and Technology, Kadapa, Andhra Pradesh 516003, India*

[3]*Faculty of Engineering, Kuwait College of Science and Technology, Doha District, Kuwait*

[4]*Center of Excellence in Desalination Technology, King Abdulaziz University, P.O. Box 80200, Jeddah 21589, Saudi Arabia*

*Address all correspondence to: M. Veera Krishna, Department of Mathematics, Rayalaseema University, Kurnool, Andhra Pradesh 518007, India; Tel.: +91 984 965 0682; Fax: +91 851 827 2600, E-mail: veerakrishna_maths@yahoo.com

Original Manuscript Submitted: 11/22/2017; Final Draft Received: 7/13/2018

Analytical solutions of an unsteady magnetohydrodynamic (MHD) flow with heat and mass transfer characteristics of an incompressible, viscous, electrically conducting, and Boussinesq fluid over a vertical oscillating plate embedded in a Darcian porous medium in the presence of a thermal radiation are presented. The fluid considered here is a gray, absorbing/emitting radiating, but nonscattering medium. At time $t > 0$, the plate temperature and concentration near the plate are raised linearly with time t. The dimensionless governing coupled unsteady boundary layer partial differential equations are solved by the Laplace transform technique. An increase in permeability parameter (K) is found to increase fluid velocities and shear stress in the regime. Also it was found that when the conduction-radiation parameter (R) increased, the fluid velocity and the temperature profiles decreased. Applications of the study are found in materials processing and solar energy collector systems.

KEY WORDS: *absorbing/emitting radiation, Darcian porosity, shear stress, materials processing, Boussinesq approximation*

1. INTRODUCTION

In recent years, the problems of free convective and heat transfer flows through a porous medium under the influence of a magnetic field have attracted the attention of a number of researchers because of their possible applications in many branches of science and technology, e.g., transportation cooling of reentry vehicles and rocket boosters, cross-hatching on ablative surfaces, and film vaporization in combustion chambers. On the other hand, flow through a porous medium has numerous engineering and geophysical applications, such as in the chemical engineering filtration and purification process; in agricultural engineering, in studying underground water resources; and in petroleum technology, in studying the movement of natural gas, oil, and water through the oil reservoirs. In view of these applications, many researchers have studied magnetohydrodynamic (MHD) free convective heat and mass transfer flow in a porous medium with different configurations; some of them are Raptis and Kafoussias (1982), Sattar (1993), and Kim (2004). Jaiswal and Soundalgekar (2001) obtained an approximate solution to the problem of an unsteady flow past an infinite vertical plate with constant suction and embedded in a porous medium with oscillating plate temperature. The unsteady flow through a highly porous medium in the presence of radiation was studied by Raptis and Perdikis (2004). Ahmed (2008) investigated the effect of transverse periodic permeability oscillating with time

1091–028X/21/$35.00

NOMENCLATURE

a	spectral mean absorption coefficient of the medium
C	concentration (kg m^{-3})
C_p	specific heat at constant pressure (J kg^{-1} K)
C_w	concentration at the surface (kg m^{-3})
C_∞	concentration in the free stream (kg m^{-3})
D	chemical molecular diffusivity (m^{2}s^{-1})
g	acceleration due to gravity (m s^{-2})
Gm	mass Grashof number
Gr	thermal Grashof number
k	permeability of the porous medium
k_1	thermal conductivity (W m^{-1} K^{-1})
K	permeability parameter
M	Hartmann number
Pr	Prandtl number
q_r	radiative heat flux
R	radiation conduction parameter
Sc	Schmidt number
T	temperature (K)
t	dimensionless time
T_w	fluid temperature at the surface (K)
T_∞	fluid temperature in the free stream (K)
(u, v)	velocity components along (x, y)-directions
u	dimensionless velocity component in x-direction (m s^{-1})
U_0	dimensionless plate velocity (m s^{-1})
v	dimensionless velocity component in y-direction (m s^{-1})

Greek Symbols

β	coefficient of volume expansion for heat transfer (K^{-1})
θ	dimensionless fluid temperature (K)
ν	kinematic viscosity (m^2 s^{-1})
ρ	density (kg m^{-3})
σ	electrical conductivity (S m^{-1})
σ_1	Stefan–Boltzmann constant
τ	shearing stress (N m^{-2})
ϕ	dimensionless concentration (kg m^3)

Subscripts

w	conditions on the wall
∞	free stream conditions

on the heat transfer flow of a viscous incompressible fluid through a highly porous medium bounded by an infinite, vertical, porous plate, by means of the series solution method. Ahmed (2010) studied the effect of transverse periodic permeability oscillating with time on the free convective heat transfer flow of a viscous, incompressible fluid through a highly porous medium bounded by an infinite, vertical, porous plate subjected to a periodic suction velocity. Kumar and Verma (2011) presented the problem of an unsteady flow past an infinite, vertical, permeable plate with constant suction and a transverse magnetic field with oscillating plate temperature. If the temperature of the surrounding fluid is high, radiation effects play an important role, and this situation does not exist in space technology. In such cases one has to take into account the effect of thermal radiation and mass diffusion. The effects of radiation and viscous dissipation on the transient natural convection-radiation flow of viscous dissipation fluid along an infinite vertical surface embedded in a porous medium, by means of the network simulation method, is investigated by Zueco (2008). The effect of radiation on the natural convection flow of a Newtonian fluid along a vertical surface embedded in a porous medium was presented by Mahmoud and Chamkha (2010). Soundalgekar and Takhar (1993) have considered the radiation free convection flow of an optically thin, gray gas past a semi-infinite vertical plate. Radiation effects on a mixed convection flow along an isothermal vertical plate were studied by Hossain and Takhar (1996).

In all the above studies, the vertical plate has been considered as stationary. Raptis and Perdikis (1999) studied the effects of thermal radiation and free convection flow past a moving vertical plate. The governing equations were solved analytically. Ahmed (2010) studied the effects of radiation and magnetic Prandtl number on the steady mixed convective heat and mass transfer flow of an optically thin, gray gas over an infinite, vertical, porous plate with constant suction in the presence of a transverse magnetic field. Ahmed (2012) investigated the effects of radiation and

viscous dissipation heat on a MHD steady mixed convective heat and mass transfer flow over an infinite, vertical, porous plate with constant suction, taking into account the induced magnetic field. Ahmed and Kalita (2012a) investigated the effects of porosity and MHD on a horizontal channel flow of a viscous, incompressible, electrically conducting fluid through a porous medium in the presence of thermal radiation and a transverse magnetic field. Ahmed and Kalita (2012b) presented the magnetohydrodynamic transient convective radiative heat transfer in an isotropic, homogenous, porous regime adjacent to a hot vertical plate. Ahmed and Kalita (2013) investigated the effects of chemical reaction as well as magnetic field on the heat and mass transfer of Newtonian fluids over an infinite, vertical oscillating plate with variable mass diffusion. Ahmed et al. (2014) gave a numerical solution for the problem of MHD heat and mass transfer flow past an impulsively started semi-infinite vertical plate in the presence of thermal radiation by an implicit finite-difference scheme of the Crank–Nicolson type. The effects of Darcian drag force and radiation conduction on the unsteady two-dimensional MHD flow of a viscous, electrically conducting, and Newtonian fluid over a vertical plate adjacent to a Darcian regime in the presence of thermal radiation and a transverse magnetic field were reported by Ahmed et al. (2014a). Ahmed (2014) analyzed the effects of conduction-radiation, porosity, and chemical reaction on the unsteady hydromagnetic free convection flow past an impulsively started semi-infinite vertical plate embedded in a porous medium in the presence of a first-order chemical reaction and thermal radiation. The boundary layer equations have been solved by an implicit finite-difference scheme of the Crank–Nicolson type, which is efficient, accurate, extensively validated, and unconditionally stable. Kumar (2013) investigated a new approximate method, namely, the homotopy perturbation transform method (HPTM), which is a combination of the homotopy perturbation method (HPM) and the Laplace transform method (LTM), to provide an analytical approximate solution to the time-fractional Cauchy-reaction diffusion equation. The problem of a non-Newtonian plane Couette flow, fully developed plane Poiseuille flow, and Couette–Poiseuille flow was presented by Ellahi and Hameed (2012). The effects of heat and mass transfer with slip on the Couette and generalized Couette flow in a homogeneous and thermodynamically compatible third-grade non-Newtonian viscous fluid and the exact solutions of velocity and temperature in the Couette flow problem were derived by Ellahi et al. (2012). Ahmed et al. (2014b) studied the oscillatory hydromagnetic flow of a viscous, incompressible, electrically conducting, non-Newtonian fluid in an inclined, rotating channel with nonconducting walls, incorporating coupled stress effects. Zueco et al. (2014) investigated the 2-D steady state boundary layer flow and heat transfer of an electrically conducting, incompressible, micropolar fluid over a continuously moving, stretching surface embedded in a Darcian porous medium with a uniform magnetic field imposed in the direction normal to the surface, and the stretching velocity is assumed to vary linearly with the distance along the sheet. Ibrahim et al. (2008) analyzed the effects of radiation absorption, mass diffusion, chemical reaction, and heat source parameter of heat generating fluid past a vertical porous plate subjected to variable suction, and they have assumed that the plate is embedded in a uniform porous medium and moves with a constant velocity in the flow direction in the presence of a transverse magnetic field. The influence of thermal radiation and first-order chemical reaction on unsteady MHD convective flow, heat and mass transfer of a viscous, incompressible, electrically conducting fluid past a semi-infinite vertical flat plate in the presence of a transverse magnetic field under oscillatory suction and a heat source in a slip-flow regime was studied by Pal and Talukdar (2012). Ahmed et al. (2015) discussed numerical and analytical solutions for MHD radiating heat/mass transport in a Darcian porous regime bounded by an oscillating vertical surface.

Khan et al. (2017a) discussed the doubly stratified flow of an Eyring–Powell nanomaterial with heat generation/absorption. Hayat et al. (2018) investigated entropy generation in MHD radiative flow due to a rotating disk. Hayat et al. (2017a) discussed the squeezing flow of a second-grade liquid subject to a non-Fourier heat flux and heat generation/absorption. Temperature-dependent thermal conductivity in stagnation point flow toward a nonlinear stretched surface with variable thickness is considered by Hayat et al. (2016). Recently, the Cattaneo–Christov heat flux model was employed by Hayat et al. (2017b) for heat transfer in the stagnation point flow due to a stretching cylinder. Numerical simulations of natural convection heat and mass transfer in a square cavity using Comsol Multiphysics 5.0 software are presented by Zeidan et al. (2016). The generalized Fourier's and Fick's laws are employed for heat and mass transfer in stagnation point flow of Powell–Eyring liquid by Waqas et al. (2017). Veera Krishna and Gangadhar Reddy (2018) discussed the unsteady MHD free convection in the boundary layer flow of an electrically conducting fluid through a porous medium subject to a uniform transverse magnetic field over a moving infinite vertical plate in the presence of a heat source and chemical reaction. Veera Krishna and Subba Reddy (2018a) have

investigated the simulation on the MHD forced convective flow through a stumpy, permeable, porous medium (oil sands, sand) using the lattice Boltzmann method. Veera Krishna and Jyothi (2018) discussed the Hall effects on an MHD rotating flow of a viscoelastic fluid through a porous medium over an infinite oscillating porous plate with a heat source and chemical reaction. Recently, Veera Krishna and Swarnalathamma (2016), Swarnalathamma and Veera Krishna (2016), Veera Krishna and Gangadhar Reddy (2016), and Veera Krishna and Subba Reddy (2016) discussed the MHD flows of an incompressible and electrically conducting viscous fluid through a porous medium in planar channels. Veera Krishna et al. (2018a) discussed heat and mass transfer on unsteady MHD oscillatory flow of blood through a porous arteriole. The effects of radiation and Hall current on an unsteady MHD free convective flow in a vertical channel filled with a porous medium have been studied by Veera Krishna et al. (2018b). MHD two-dimensional flow of an incompressible Burgers material bounded by a permeable, stretched surface is addressed by Hayat et al. (2017c). The characteristics of Newtonian heating on a permeable, stretched flow of a viscous nano-material are investigated by Hayat et al. (2017d). Khan et al. (2017b) discussed the MHD stagnation point flow of Casson fluid toward a stretching sheet. Veera Krishna and Chamkha (2018) investigated the Hall effects on the unsteady MHD flow of second-grade fluid through a porous medium with ramped wall temperature and ramped surface concentration. Veera Krishna et al. (2018c) investigated heat and mass transfer on an MHD free convective flow over an infinite, nonconducting, vertical, flat, porous plate. Veera Krishna et al. (2018d) discussed heat and mass transfer on the unsteady MHD oscillatory flow of second-grade fluid through a porous medium between two vertical plates under the influence of a fluctuating heat source/sink and a chemical reaction.

Veera Krishna and Chamkha (2019a) discussed the MHD squeezing flow of a water-based nanofluid through a saturated porous medium between two parallel disks, taking the Hall current into account. Veera Krishna and Chamkha (2019b) investigated The diffusion-thermo, radiation-absorption and Hall and ion slip effects on MHD free convective rotating flow of nano-fluids past a semi-infinite permeable moving plate with constant heat source. Hall and ion slip effects on Unsteady MHD Convective Rotating flow of Nanofluids have been discussed by Veera Krishna and Chamkha (2020a). Veera Krishna and Chamkha (2020b) investigated the Hall and ion slip effects on the MHD convective flow of elastico-viscous fluid through porous medium between two rigidly rotating parallel plates with time fluctuating sinusoidal pressure gradient. Veera Krishna et al. (2020a) investigated the Hall and ion slip effects on the unsteady MHD free convective rotating flow through porous medium past an exponentially accelerated inclined plate. The combined effects of Hall and ion slip on MHD rotating flow of ciliary propulsion of microscopic organism through porous medium have been studied by Veera Krishna et al. (2020b). Veera Krishna et al. (2020c) discussed the MHD flow of an electrically conducting second-grade fluid through porous medium over a semi-infinite vertical stretching sheet. The influence of thermal radiation, Hall and ion-slip impacts on the unsteady MHD free convective rotating flow of Jeffreys fluid past an infinite vertical porous plate with the ramped wall temperature has been investigated by Veera Krishna (2020).

In this paper, the effects of porosity of the porous medium and radiation conduction on the heat and mass transfer of Newtonian fluids over an infinite, vertical, oscillating permeable plate immersed in a saturated porous medium with variable mass diffusion have been considered.

2. FORMULATION AND SOLUTION OF THE PROBLEM

The unsteady MHD laminar boundary layer flow of a viscous, incompressible Newtonian fluid passed along an infinite, vertical, oscillating plate embedded in a saturated porous medium with variable temperature and also with mass diffusion in the presence of a transverse applied magnetic field and thermal radiation has been considered in Fig. 1. The x axis is taken along the plate in the vertical upward direction, and the z axis is taken normal to the plate. Initially it is assumed that the plate and fluid are at the same temperature T_∞ in the stationary condition, with concentration level C_∞ at all the points. At time $t > 0$ the plate is given an oscillatory motion in its own plane with velocity $U_0 e^{i\omega t}$. At the same time, the plate temperature is raised linearly with time t, and mass is also diffused from the plate linearly with time.

A transverse magnetic field of uniform strength B_0 is assumed to be applied normal to the plate. As the magnetic Reynolds number of the flow is very low, the induced magnetic field and viscous dissipation are assumed to be negligible. The fluid considered here is gray and absorbs/emits radiation but is a nonscattering medium. Then, by the

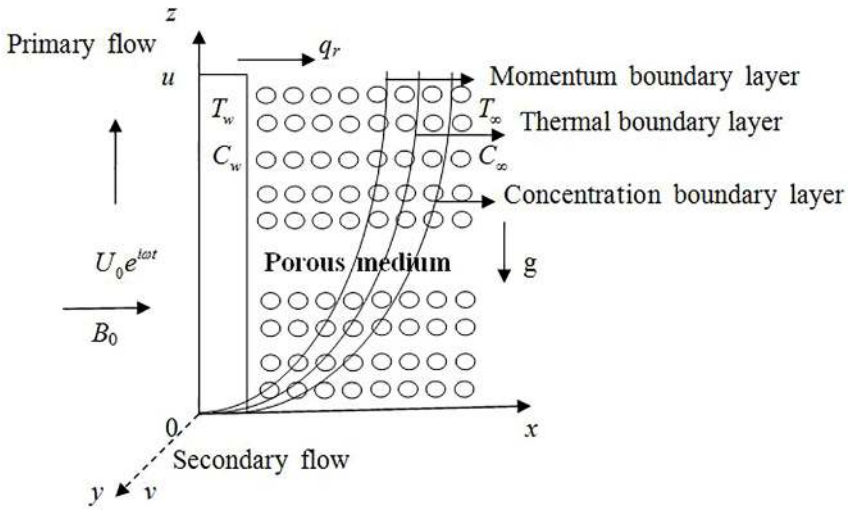

FIG. 1: Physical configuration of the problem

usual Boussinesq approximation, the unsteady flow is governed by the following equations:

$$\frac{\partial u}{\partial t} = \nu \frac{\partial^2 u}{\partial z^2} - \left(\frac{\sigma B_0^2}{\rho} + \frac{\nu}{k} \right) u + g\beta \left(T - T_\infty \right) + g\beta * \left(C - C_\infty \right), \tag{1}$$

$$\frac{\partial v}{\partial t} = \nu \frac{\partial^2 v}{\partial z^2} - \left(\frac{\sigma B_0^2}{\rho} + \frac{\nu}{k} \right) v, \tag{2}$$

$$\rho C_p \frac{\partial T}{\partial t} = k_1 \frac{\partial^2 T}{\partial z^2} - \frac{\partial q_r}{\partial z}, \tag{3}$$

$$\frac{\partial C}{\partial T} = D \frac{\partial^2 C}{\partial z^2}. \tag{4}$$

The initial and boundary conditions are as follows:

$$\begin{gathered} u = 0, \quad v = 0, \quad T = T_\infty, \quad C = C_\infty \quad t \leq 0, \quad \forall \quad z \\ u = U_0 e^{i\omega t}, \quad v = 0, \quad T = T_\infty + (T_w - T_\infty) At, \quad C = C_\infty + (C_w - C_\infty) At, \quad \text{for} \quad t > 0, \quad z = 0, \\ u \to 0, \quad v \to 0, \quad T \to T_\infty, \quad C \to C_\infty \quad \text{for} \quad t > 0, \qquad \text{as} \qquad z \to \infty. \end{gathered} \tag{5}$$

Combining Eqs. (1) and (2), let $q = u + iv$, it is obtained as,

$$\frac{\partial q}{\partial t} = \nu \frac{\partial^2 q}{\partial z^2} - \left(\frac{\sigma B_0^2}{\rho} + \frac{\nu}{k} \right) q + g\beta \left(T - T_\infty \right) + g\beta^* \left(C - C_\infty \right). \tag{6}$$

The local radiant absorption for the case of an optically thin, gray gas is expressed as

$$\frac{\partial q_r}{\partial z} = -4a\sigma \left(T_\infty^4 - T^4 \right). \tag{7}$$

Following Raptis and Perdikis (2004) and Ahmed (2010, 2012), we assume that the temperature differences within the flow are sufficiently small, so that T^4 can be expressed as a linear function of T after using Taylor's series to expand T^4 about the free stream temperature T_∞ and neglecting higher-order terms. This results in the following approximation:

$$T^4 \cong 4T_\infty^3 T - 3T_\infty^4, \tag{8}$$

$$\rho C_p \frac{\partial T}{\partial t} = k_1 \frac{\partial^2 T}{\partial z^2} - 16a\sigma_1 T_\infty^3 \left(T - T_\infty\right). \tag{9}$$

We introduce the following nondimensional quantities:

$$\begin{gathered} z^* = \frac{w_0 z}{\nu}, \quad q^* = \frac{q}{U_0}, \quad \theta = \frac{T - T_\infty}{T_w - T_\infty}, \quad \phi = \frac{C - C_\infty}{C_w - C_\infty}, \quad \mathrm{Sc} = \frac{\nu}{D}, \quad \mathrm{Pr} = \frac{\rho \nu C_p}{k_1}, \\ K = \frac{U_0^2 k}{\nu^2}, \quad A = \frac{U_0^2}{\nu}, \quad \mathrm{Gr} = \frac{\nu g \beta \left(T_w - T_\infty\right)}{U_0^3}, \\ \mathrm{Gm} = \frac{\nu g \beta \left(C_w - C_\infty\right)}{U_0^3}, \quad t^* = \frac{U_0^2 t}{\nu}, \quad M^2 = \frac{\sigma B_0^2 \nu}{\rho U_0^2}, \quad R = \frac{16a\nu\sigma T_\infty^3}{k_1 U_0^2}. \end{gathered} \tag{10}$$

Using the transformations of Eq. (10), the nondimensional forms of Eqs. (1), (4), and (9) are (dropping asterisks),

$$\frac{\partial q}{\partial t} = \frac{\partial^2 q}{\partial z^2} - \left(M^2 + \frac{1}{K}\right) q + \mathrm{Gr}\theta + \mathrm{Gm}\phi, \tag{11}$$

$$\frac{\partial \theta}{\partial t} = \frac{1}{\mathrm{Pr}} \frac{\partial^2 \theta}{\partial z^2} - \frac{R}{\mathrm{Pr}} \theta, \tag{12}$$

$$\frac{\partial \phi}{\partial t} = \frac{1}{\mathrm{Sc}} \frac{\partial^2 \phi}{\partial z^2}. \tag{13}$$

The corresponding initial and boundary conditions are

$$\begin{gathered} q = 0, \quad \theta = 0, \quad \phi = 0, \quad t \le 0, \quad \forall \quad z \\ q = e^{i\omega t}, \quad \theta = 1, \quad \phi = t, \quad t > 0 \quad \text{at} \quad z = 0, \\ q \to 0, \qquad \theta \to 0, \quad \phi \to 0, \quad t > 0 \quad \text{as} \quad z \to \infty. \end{gathered} \tag{14}$$

The unsteady coupled partial differential equations [Eqs. (11)–(13)] along with their boundary conditions [Eq. (14)] have been solved analytically using the Laplace transform technique, and the solutions of concentration, temperature and velocity distributions for MHD flow in the presence of radiation and porous medium are obtained as follows:

$$\phi = t\left(\left(1 + 2\eta^2 \mathrm{Sc}\right) erfc\left(\eta\sqrt{\mathrm{Sc}}\right) - \frac{2\eta\sqrt{\mathrm{Sc}}}{\sqrt{\pi}} \exp\left(-\eta^2 \mathrm{Sc}\right)\right), \tag{15}$$

$$\begin{aligned} \theta = {} & \left(\frac{t}{2} + \frac{z\mathrm{Pr}}{4\sqrt{R}}\right) \exp\left(z\sqrt{R}\right) erfc\left(\eta\sqrt{\mathrm{Pr}} + \sqrt{\frac{Rt}{\mathrm{Pr}}}\right) \\ & + \left(\frac{t}{2} - \frac{z\mathrm{Pr}}{4\sqrt{R}}\right) \exp\left(-z\sqrt{R}\right) erfc\left(\eta\sqrt{\mathrm{Pr}} - \sqrt{\frac{Rt}{\mathrm{Pr}}}\right), \end{aligned} \tag{16}$$

$$
\begin{aligned}
q = {} & \frac{1}{4}\exp(i\omega t)\left[\exp\left(z\sqrt{N+i\omega}\right) erfc\left\{\eta+\sqrt{(N+i\omega)\,t}\right\}+\exp\left(-z\sqrt{N+i\omega}\right)\right.\\
& \left.\times\, erfc\left\{\eta-\sqrt{(N+i\omega)\,t}\right\}\right]+\frac{1}{4}\exp(-i\omega t)\left[\exp\left(z\sqrt{N-i\omega}\right) erfc\left\{\eta+\sqrt{(N-i\omega)\,t}\right\}\right.\\
& \left.+\exp\left(-z\sqrt{N-i\omega}\right) erfc\left\{\eta-\sqrt{(N-i\omega)\,t}\right\}\right]\\
& +B\left[\left(\frac{t}{2}+\frac{z}{4\sqrt{N}}\right)\exp\left(z\sqrt{N}\right) erfc\left(\eta+\sqrt{Nt}\right)+\left(\frac{t}{2}-\frac{z}{4\sqrt{N}}\right)\exp\left(-z\sqrt{N}\right) erfc\left(\eta-\sqrt{Nt}\right)\right]\\
& +\frac{E}{2}\exp(-Ct)\left[\exp\left(z\sqrt{N-C}\right) erfc\left\{\eta+\sqrt{(N-c)\,t}\right\}+\exp\left(-z\sqrt{N-C}\right)\right.\\
& \left.\times\, erfc\left\{\eta-\sqrt{(N-C)\,t}\right\}\right]+\frac{G}{2}\exp(et)\left[\exp\left(z\sqrt{N+e}\right) erfc\left\{\eta+\sqrt{(N+e)\,t}\right\}\right.\\
& \left.+\exp\left(-z\sqrt{N+e}\right) erfc\left\{\eta-\sqrt{(N+e)\,t}\right\}\right]+\frac{E}{2}\left[\exp\left(z\sqrt{R}\right) erfc\left(\eta\sqrt{\mathrm{Pr}}+\sqrt{\frac{Rt}{\mathrm{Pr}}}\right)\right.\\
& \left.+\exp\left(-z\sqrt{R}\right) erfc\left(\eta\sqrt{\mathrm{Pr}}-\sqrt{\frac{Rt}{\mathrm{Pr}}}\right)\right]+D\theta(z,t)+F\phi(z,t)\\
& +\frac{E}{2}\exp(-Ct)\left[\begin{array}{l}\exp\left(z\sqrt{R-C\mathrm{Pr}}\right) erfc\left\{\eta\sqrt{\mathrm{Pr}}+\sqrt{\left(\frac{R}{\mathrm{Pr}}-C\right)t}\right\}\\ +\exp\left(-z\sqrt{R-C\mathrm{Pr}}\right) erfc\left\{\eta\sqrt{\mathrm{Pr}}-\sqrt{\left(\frac{R}{\mathrm{Pr}}-C\right)t}\right\}\end{array}\right]\\
& +Ge\,rfc\left(\eta\sqrt{\mathrm{Sc}}\right)-\frac{G}{2}\left[\exp\left(z\sqrt{e\mathrm{Sc}}\right) erfc\left(\eta\sqrt{\mathrm{Sc}}+\sqrt{et}\right)+\exp\left(-z\sqrt{e\mathrm{Sc}}\right) erfc\left(\eta\sqrt{\mathrm{Sc}}-\sqrt{et}\right)\right],
\end{aligned}
\tag{17}
$$

where

$$
\eta=\frac{z}{2\sqrt{t}},\quad N=M^2+\frac{1}{K},\quad A=\frac{\mathrm{Gr}\,(\mathrm{Pr}-1)}{(R-N)^2}+\frac{\mathrm{Gm}\,(\mathrm{Sc}-1)}{N^2},\quad B=\frac{N\,(\mathrm{Gr}+\mathrm{Gm})-R\mathrm{Gm}}{N\,(R-N)},
$$

$$
C=\frac{R-N}{\mathrm{Pr}-1},\quad D=\frac{\mathrm{Gr}}{R-N},\quad e=\frac{N}{\mathrm{Sc}-1},\quad E=\frac{\mathrm{Gr}\,(\mathrm{Pr}-1)}{(R-N)^2},\quad F=\frac{\mathrm{Gm}}{N},\quad \text{and}\quad G=\mathrm{Gm}\left(\frac{\mathrm{Sc}-1}{N}\right)^2.
$$

The boundary layer produces a drag force on the plate due to the viscous stresses that are developed at the wall. The viscous stress at the surface of the plate is given by

$$
\tau=-\left[\frac{\partial q(z,t)}{\partial z}\right]_{z=0}=-\frac{1}{2\sqrt{t}}\left[\frac{\partial q(z,t)}{\partial \eta}\right]_{\eta=0}. \tag{18}
$$

The Nusselt number can be obtained by the following formula:

$$
\mathrm{Nu}=-\left(\frac{\partial\theta}{\partial z}\right)_{z=0}=-\frac{1}{2\sqrt{t}}\left(\frac{\partial\theta}{\partial\eta}\right)_{\eta=0}. \tag{19}
$$

The Sherwood number can be obtained by the following formula:

$$
\mathrm{Sh}=-\left(\frac{\partial\phi}{\partial z}\right)_{z=0}=-\frac{1}{2\sqrt{t}}\left(\frac{\partial\phi}{\partial\eta}\right)_{\eta=0}=2\sqrt{\frac{t\mathrm{Sc}}{\pi}}. \tag{20}
$$

3. RESULTS AND DISCUSSION

To expand a viewpoint of the physics of the flow regime, we have numerically evaluated the effects of the Hartmann number (M), Grashof number (Gr), radiation conduction parameter (R), dimensionless time (t), and porosity parameter (K) on the velocity components u and v, temperature θ, concentration ϕ, shear stress, Nusselt number, and

Sherwood number. Here we consider Gr $= 3$, Gm $= 5 > 0$ (cooling of the plate), i.e., free convection currents convey heat away from the plate into the boundary layer, and $t = 1$, $R = 1$ throughout the discussion. To ascertain the accuracy of the numerical results, the present study is compared with the previous study. The velocity and concentration profiles are compared with the available solutions of Jaiswal and Soundalgekar (2001) and Kumar and Verma (2011). It is observed that the present results are in good agreement with them. Figures 2 and 3, Figs. 4–6, and Figs. 7–22 represent the concentration, temperature, and velocity components for u and v, respectively. The skin friction, Nusselt number, and Sherwood number at the plate are evaluated numerically and discussed with governing parameters and are tabulated in Tables 1–3. Fixing the parameters $M = 2$, $K = 1$, Pr = 0.71, $R = 1$, Sc = 0.22, Gr = 3, Gm = 5, and $\omega = \pi/6$, we draw the profiles, varying for each parameter while the other parameters are fixed.

It is noted in Fig. 2 that the concentration at all points in the flow field decreases exponentially with z and tends to zero as $z \to 10$. A comparison of curves in the figure shows a decrease in concentration with an increase in Schmidt number (Sc). Physically it is true, since the increase of Sc means the decrease of molecular diffusivity and therefore decreases in concentration at the boundary layer. Hence, the concentration of species is higher for small values of Sc and lower for large values of Sc. On the other hand, the concentration is found to escalate with time t (Fig. 3). Figure 4 reveals the transient temperature profiles against z (distance from the plate). The magnitude of temperature is maximum at the plate and then asymptotically decays to zero. The magnitude of temperature for air (Pr = 0.71) is greater than that of water (Pr = 7). This is due to the fact that the thermal conductivity of fluid decreases with increasing Pr, resulting in a decrease in thermal boundary layer thickness. As R increases, considerable reduction is observed in temperature profiles from the peak value at the wall ($z = 0$) across the boundary layer regime to the

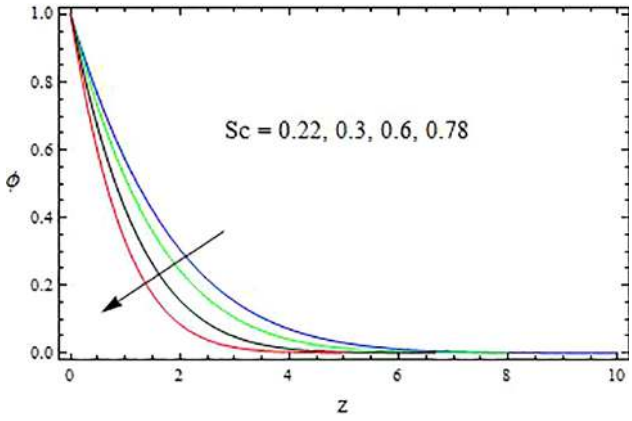

FIG. 2: The concentration profile for ϕ against Sc with $t = 1$

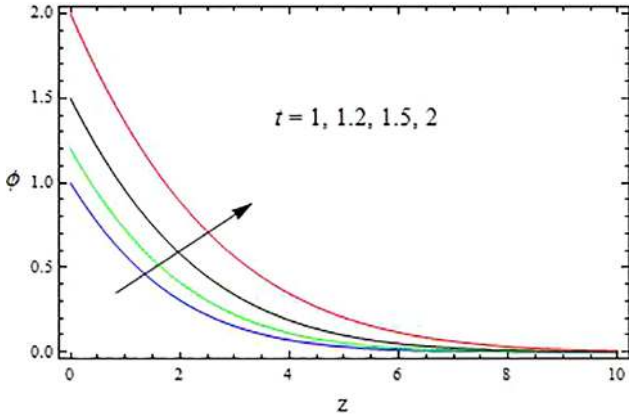

FIG. 3: The concentration profile for ϕ against t with Sc $= 0.22$

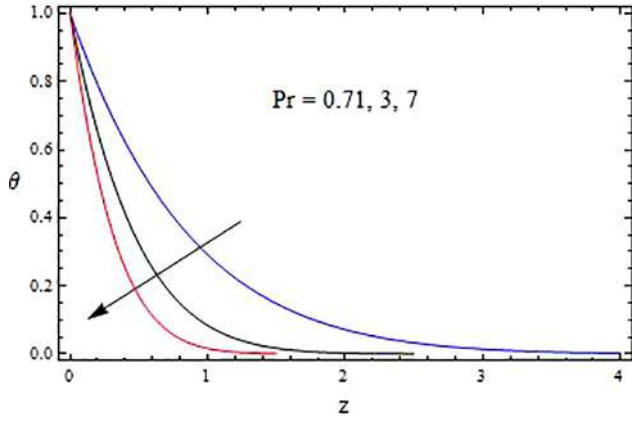

FIG. 4: The temperature profile for θ against Pr with $R = 0.5, t = 1$

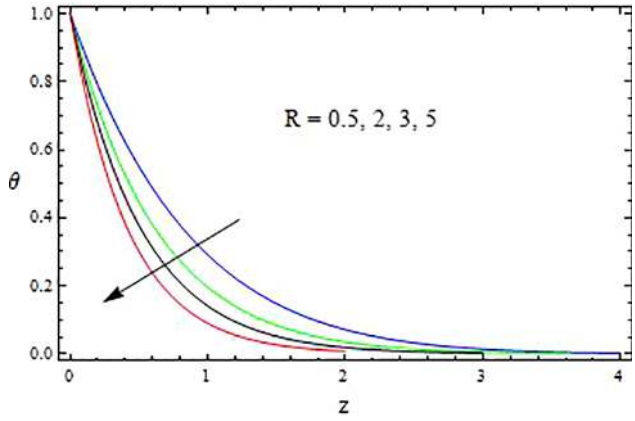

FIG. 5: The temperature profile for θ against R with $\text{Pr} = 0.71, t = 1$

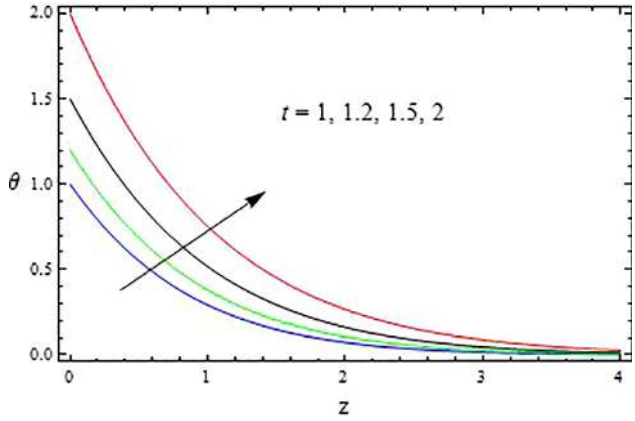

FIG. 6: The temperature profile for θ against t with $\text{Pr} = 0.71, R = 0.5$

free stream, at which temperature is negligible for any value of R (Fig. 5). It is also observed that the reduction in temperature is accompanied by simultaneous reductions in the thermal boundary layer. Temperature increases with an increase in time parameter t (Fig. 6). All profiles decay asymptotically to zero in the free stream. This is in accordance with the results of Mahmoud and Chamkha (2010) and Raptis and Perdikis (1999).

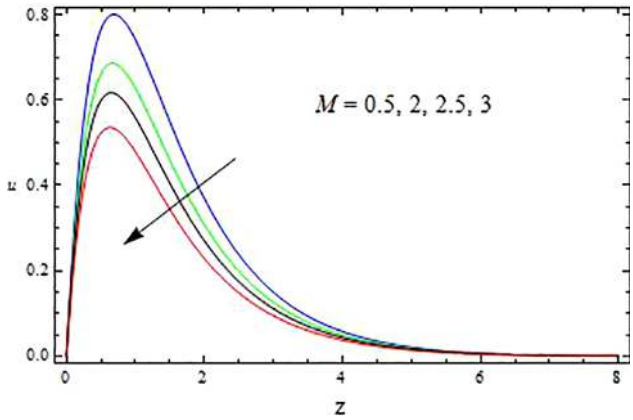

FIG. 7: The velocity profile for u against M with $K = 0.5, \text{Gr} = 3, \text{Gm} = 5, \text{Pr} = 0.71, R = 1, \text{Sc} = 0.22, \omega t = \pi/2, t = 1$

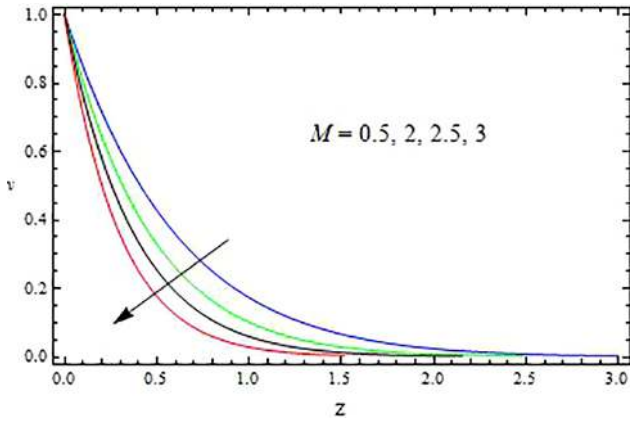

FIG. 8: The velocity profile for v against M with $K = 0.5, \text{Gr} = 3, \text{Gm} = 5, \text{Pr} = 0.71, R = 1, \text{Sc} = 0.22, \omega t = \pi/2, t = 1$

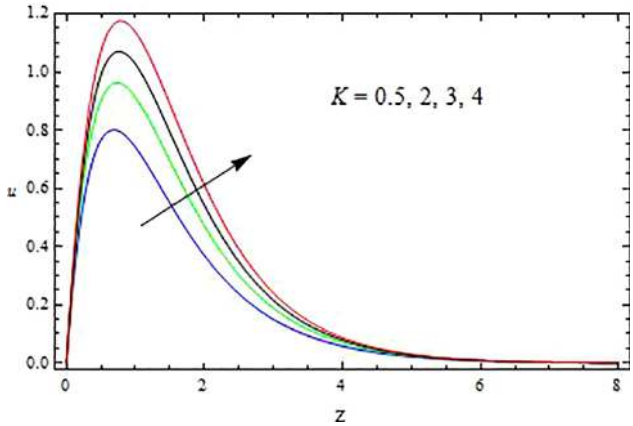

FIG. 9: The velocity profile for u against K with $M = 0.5, \text{Gr} = 3, \text{Gm} = 5, \text{Pr} = 0.71, R = 1, \text{Sc} = 0.22, \omega t = \pi/2, t = 1$

We noticed from Figs. 7 and 8 that both velocity components u and v retard with increasing the intensity of the magnetic field (Hartmann number M). It is obvious that an increase in the local magnetic parameter M results in a decrease in the velocity at all points. The application of a transverse magnetic field on an electrically conducting fluid gives rise to a resistive type of force called the Lorentz force. This force has the propensity to reduce speed for

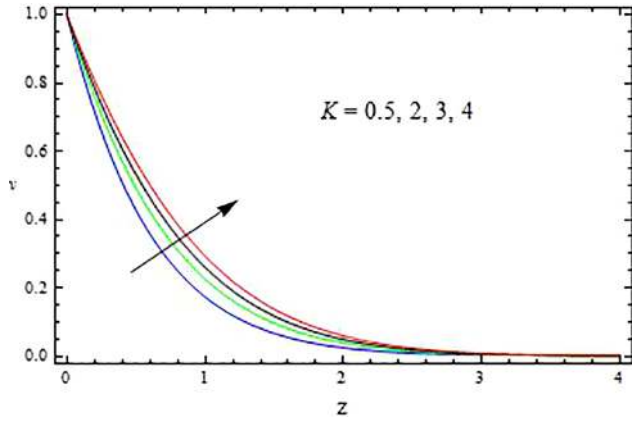

FIG. 10: The velocity profile for v against K with $M = 0.5, \text{Gr} = 3, \text{Gm} = 5, \text{Pr} = 0.71, R = 1, \text{Sc} = 0.22, \omega t = \pi/2, t = 1$

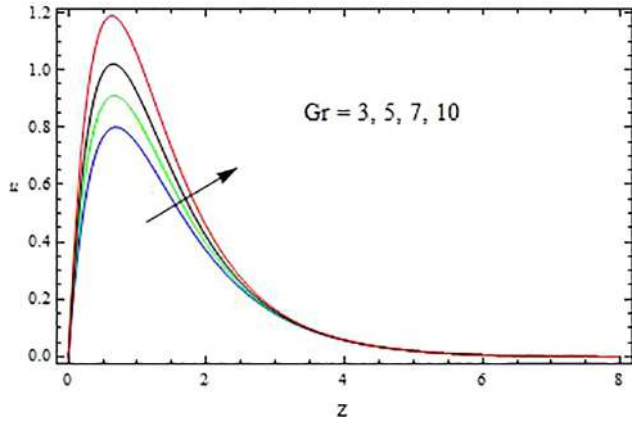

FIG. 11: The velocity profile for u against Gr with $M = 0.5, K = 0.5, \text{Gm} = 5, \text{Pr} = 0.71, R = 1, \text{Sc} = 0.22, \omega t = \pi/2, t = 1$

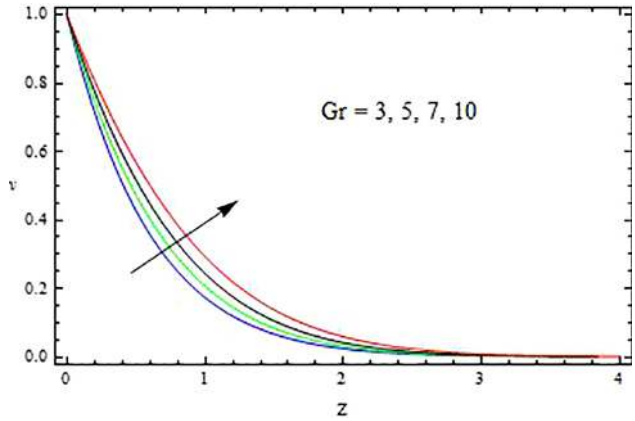

FIG. 12: The velocity profile for v against Gr with $M = 0.5, K = 0.5, \text{Gm} = 5, \text{Pr} = 0.71, R = 1, \text{Sc} = 0.22, \omega t = \pi/2, t = 1$

the motion of the fluid in the boundary layer. Figures 9 and 10 depict the variation of the velocity components with permeability parameter K. Both velocity components u and v enhance with the increase of permeability parameter K. The lower the permeability of the porous medium, the lesser the fluid speed in the entire fluid medium. The presence of a porous medium increases the resistance to flow, resulting in a decrease in the flow velocity. This behavior is depicted

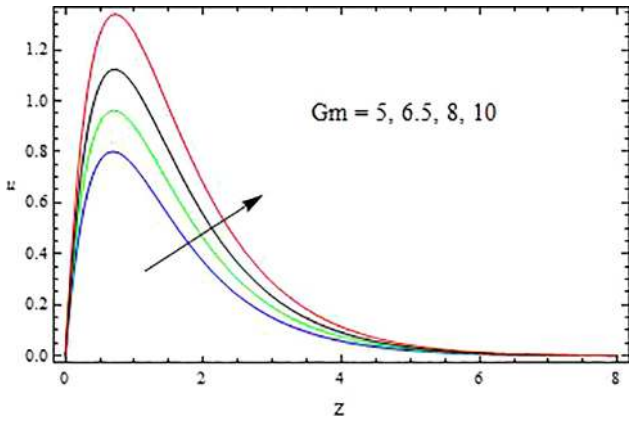

FIG. 13: The velocity profile for u against Gm with $M = 0.5, K = 0.5, \text{Gr} = 3, \text{Pr} = 0.71, R = 1, \text{Sc} = 0.22, \omega t = \pi/2, t = 1$

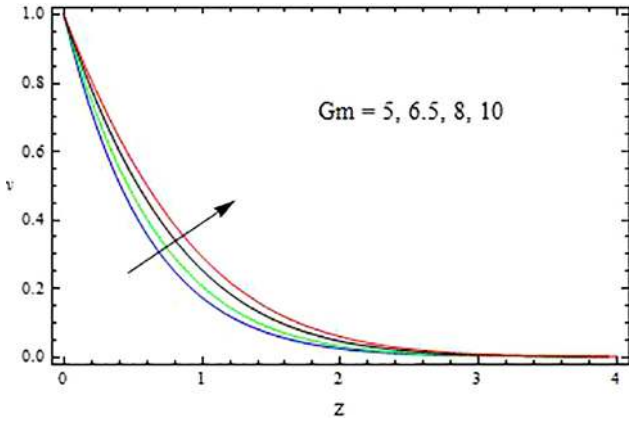

FIG. 14: The velocity profile for v against Gm with $M = 0.5, K = 0.5, \text{Gr} = 3, \text{Pr} = 0.71, R = 1, \text{Sc} = 0.22, \omega t = \pi/2, t = 1$

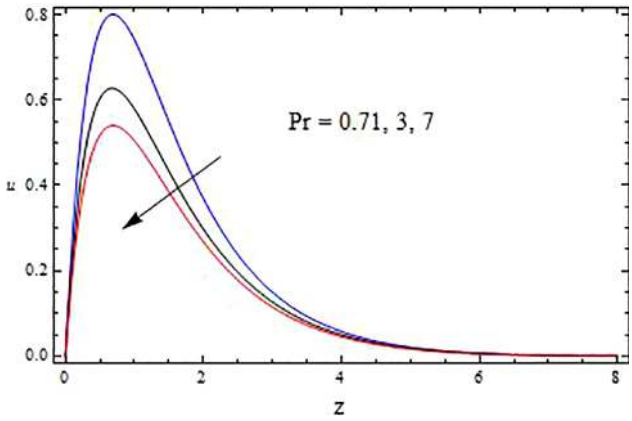

FIG. 15: The velocity profile for u against Pr with $M = 0.5, K = 0.5, \text{Gr} = 3, \text{Gm} = 5, R = 1, \text{Sc} = 0.22, \omega t = \pi/2, t = 1$

by the decrease in the velocity as K decreases. This result also corresponds to those of Jaiswal and Soundalgekar (2001) and Zueco (2008). Figures 11–14 show the effects of thermal Grashof number (Gr) and mass Grashof number (Gm) on the velocity field. We noticed that an increase in Gr results in an increase in the velocity. Similar behavior is achieved with the solutal Grashof number (Gm) on velocity.

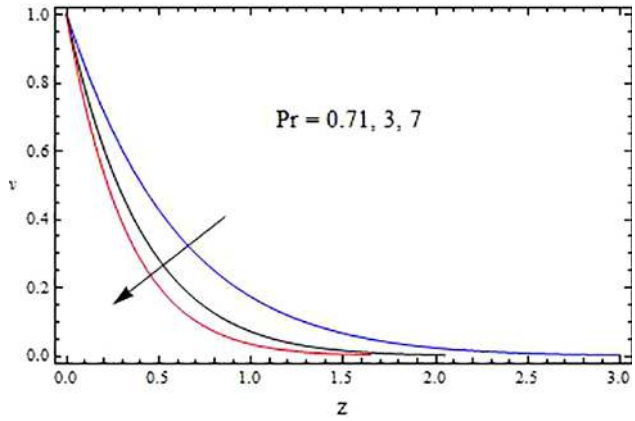

FIG. 16: The velocity profile for v against Pr with $M = 0.5, K = 0.5, \text{Gr} = 3, \text{Gm} = 5, R = 1, \text{Sc} = 0.22, \omega t = \pi/2, t = 1$

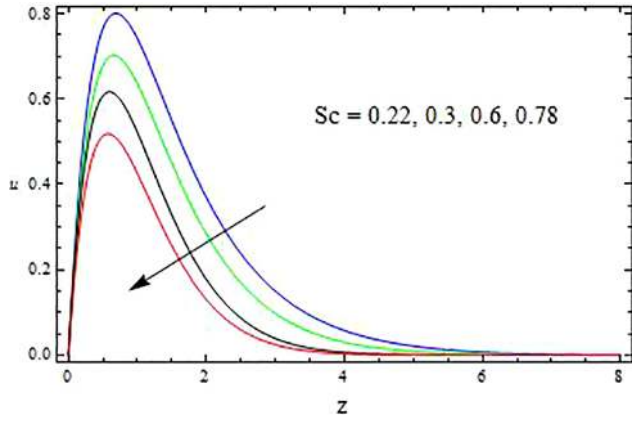

FIG. 17: The velocity profile for u against Sc with $M = 0.5, K = 0.5, \text{Gr} = 3, \text{Gm} = 5, \text{Pr} = 0.71, R = 1, \omega t = \pi/2, t = 1$

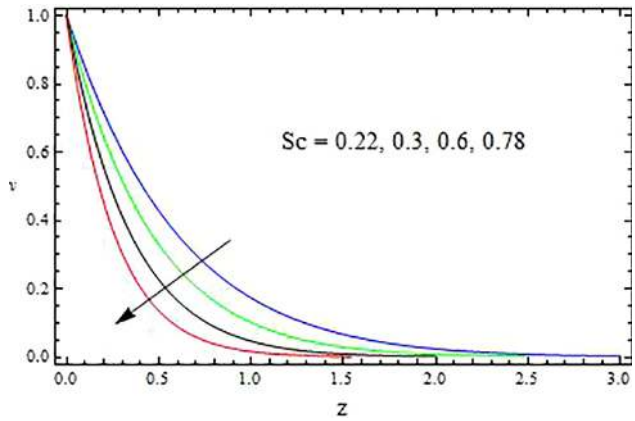

FIG. 18: The velocity profile for v against Sc with $M = 0.5, K = 0.5, \text{Gr} = 3, \text{Gm} = 5, \text{Pr} = 0.71, R = 1, \omega t = \pi/2, t = 1$

Figs. 15–20 reveal the effects of Pr, Sc, and R on the velocity profiles. It is evident from Figs. 15–16 that velocity components u and v decrease with an increase in Pr for both air and water. Furthermore, the velocity decreases and attains its minimum value in the vicinity of the plate. The magnitude of velocity for Pr = 0.71 is much higher than that of Pr = 3 and Pr = 7. Physically, this is possible because fluids with high Prandtl numbers have high viscosity and

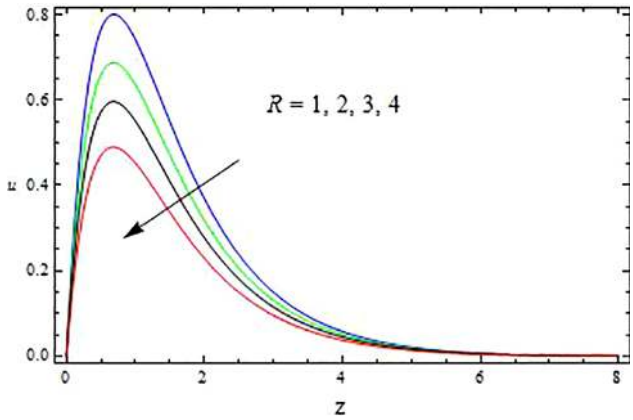

FIG. 19: The velocity profile for u against R with $M = 0.5, K = 0.5, \text{Gr} = 3, \text{Gm} = 5, \text{Pr} = 0.71, \text{Sc} = 0.22, \omega t = \pi/2, t = 1$

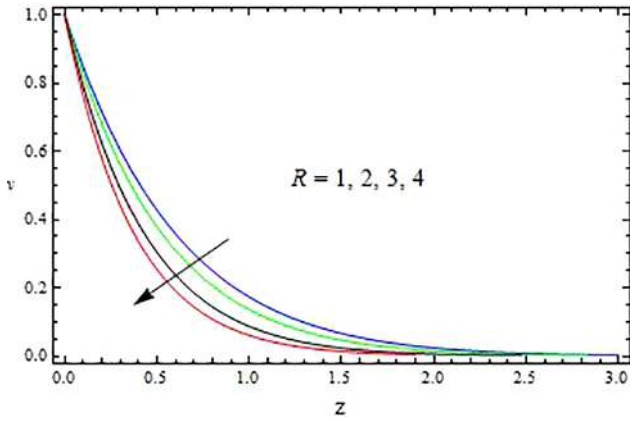

FIG. 20: The velocity profile for v against R with $M = 0.5, K = 0.5, \text{Gr} = 3, \text{Gm} = 5, \text{Pr} = 0.71, \text{Sc} = 0.22, \omega t = \pi/2, t = 1$

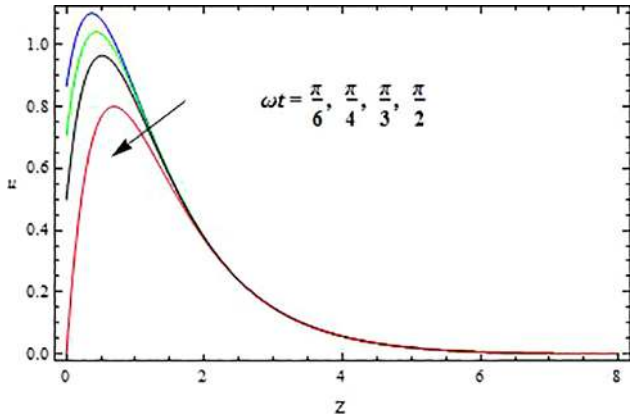

FIG. 21: The velocity profile for u against ωt with $M = 0.5, K = 0.5, \text{Gr} = 3, \text{Gm} = 5, \text{Pr} = 0.71, R = 1, \text{Sc} = 0.22, t = 1$

hence move slowly; that is, smaller values of Pr are equivalent to increasing the thermal conductivity, and therefore heat is able to diffuse away from the heated surface more rapidly than at higher values of Pr. It is evident that velocity components u and v reduce with increasing Schmidt number (Sc) or radiation conduction parameter (R) (Figs. 17–20). Finally, velocity component u decreases, and v increases, as the frequency of oscillation ωt increases (Figs. 21

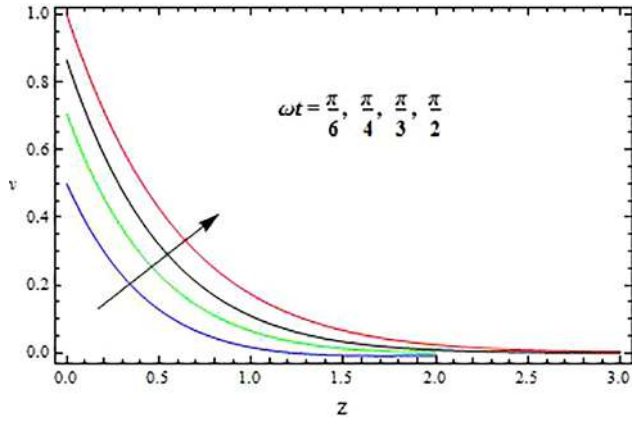

FIG. 22: The velocity profile for v against ωt with $M = 0.5, K = 0.5, \text{Gr} = 3, \text{Gm} = 5, \text{Pr} = 0.71, R = 1, \text{Sc} = 0.22, t = 1$

TABLE 1: Sherwood number

Sc	t	Sh
0.22	1	0.529257
0.3	—	0.618039
0.6	—	0.874039
0.78	—	0.996557
—	1.2	0.579772
—	1.5	0.648204
—	2	0.748482

TABLE 2: Nusselt number

Pr	R	t	Nu
0.71	0.5	1	0.049445
3	—	—	0.767206
7	—	—	2.600860
—	2	—	0.000912
—	2.5	—	0.000319
—	3	—	0.000117
—	—	1.2	0.037763
—	—	1.5	0.025826
—	—	2	0.014347

and 22). The primary velocity component u accelerated as time increased, whereas the opposite nature was observed for the secondary component v (Figs. 23 and 24).

We also noticed from Table 1 that the Sherwood number (Sh) enhances as Schmidt number (Sc) and time t increase. The Nusselt number (Nu) increases with Prandtl number (Pr) and decreases with radiation conduction parameter (R) and time (t) (Table 2). The skin friction components τ_x and τ_y enhance with increasing Prandtl number (Pr) and decrease with thermal Grashof number (Gr) and mass Grashof number (Gm). The component τ_x increases, and τ_y decreases, as Hartmann number (M) and permeability parameter (K) increase, whereas the reverse behavior is observed with increasing Sc, radiation conduction parameter (R), and frequency of oscillation ωt (Table 3). The results are compared with the results of Ahmed et al. (2015), shown in Tables 4–6.

TABLE 3: Skin friction

M	K	Gr	Gm	Pr	Sc	R	ωt	τ_x	τ_y
0.5	0.5	3	5	0.71	0.22	1	$\pi/6$	0.468552	0.052014
1	—	—	—	—	—	—	—	0.512001	0.041528
2	—	—	—	—	—	—	—	0.625663	0.032556
—	1	—	—	—	—	—	—	0.748554	0.032256
—	2	—	—	—	—	—	—	0.985547	0.024158
—	—	5	—	—	—	—	—	0.314522	0.014552
—	—	7	—	—	—	—	—	0.204520	0.008554
—	—	—	7	—	—	—	—	0.289665	0.035526
—	—	—	10	—	—	—	—	0.174485	0.024785
—	—	—	—	3	—	—	—	0.652247	0.085479
—	—	—	—	7	—	—	—	0.785985	0.141254
—	—	—	—	—	0.3	—	—	0.389665	0.085527
—	—	—	—	—	0.6	—	—	0.325585	0.126552
—	—	—	—	—	—	2	—	0.223655	0.244523
—	—	—	—	—	—	3	—	0.142254	0.452885
—	—	—	—	—	—	—	$\pi/4$	0.258898	0.096689
—	—	—	—	—	—	—	$\pi/3$	0.145258	0.254478

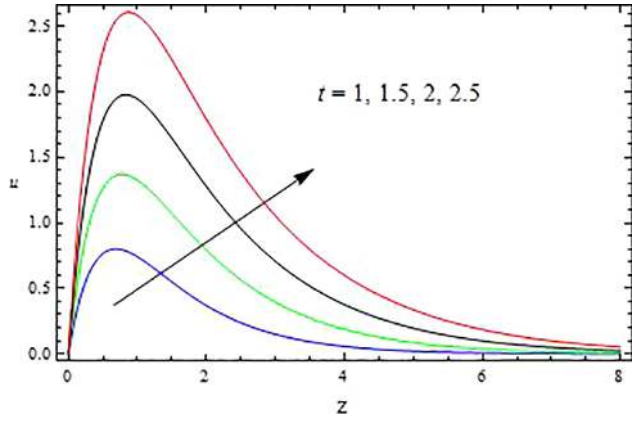

FIG. 23: The velocity profile for u against t with $M = 0.5, K = 0.5, \text{Gr} = 3, \text{Gm} = 5, \text{Pr} = 0.71, R = 1, \text{Sc} = 0.22, \omega t = \pi/2$

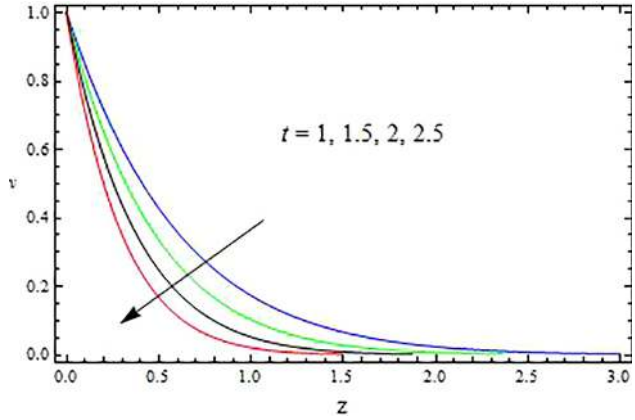

FIG. 24: The velocity profile for v against t with $M = 0.5, K = 0.5, \text{Gr} = 3, \text{Gm} = 5, \text{Pr} = 0.71, R = 1, \text{Sc} = 0.22, \omega t = \pi/2$

TABLE 4: Comparison of results for the velocity $M = 0.5, K = 0.5, \text{Sc} = 0.22, \text{Pr} = 0.71, R = 1, \text{Gm} = 5, \omega t = \pi/2, t = 1, z = 2$

Gm	Previous Results Ahmed et al. (2015) Crank–Nicolson Method	Present Results Laplace Transform Technique
5	0.384885	0.384775
7	0.432656	0.432589
10	0.548079	0.547087
12	0.632847	0.632256

TABLE 5: Comparison of results for the temperature $R = 0.5, t = 1, z = 2$

Pr	Previous Results Ahmed et al. (2015) Crank–Nicolson Method	Present Results Laplace Transform Technique
0.71	0.0711189	0.0711681
3	0.0025077	0.0025271
7	0.0000181	0.0000186

TABLE 6: Comparison of results for the concentration $t = 1, z = 2$

Sc	Previous Results Ahmed et al. (2015) Crank–Nicolson Method	Present Results Laplace Transform Technique
0.22	0.284308	0.284447
0.3	0.228051	0.228774
0.6	0.167541	0.164551
0.78	0.084308	0.081447

4. CONCLUSIONS

Transient free convection-radiation MHD viscous incompressible flow along an infinite, vertical, permeable plate immersed in a porous medium under a transverse magnetic field has been presented. A flux model has been employed to simulate the thermal radiation effects, valid for optically thick gases. The analytical solutions of the governing equations are evaluated through the Laplace transform technique under appropriate boundary conditions, and the results indicate the following:

1. The flow is generally decelerated with the increase of Hartmann number M.
2. With an increase in time, the flow, temperature, and concentration are progressively accelerated.
3. Velocity and temperature were decreased with an increase in free convection-radiation parameter.
4. Increasing porosity contribution serves to depress skin friction in magnitude significantly in the regime.
5. With an increase in Sc and time, the mass transfer coefficient is progressively accelerated.
6. Nusselt number increases with Pr and decreases with R and t.

REFERENCES

Ahmed, S., Zueco, J., and López-Ochoa, L.M., Numerical Modeling of MHD Convective Heat and Mass Transfer in Presence of First-Order Chemical Reaction and Thermal Radiation, *Chem. Eng. Commun.*, vol. **201**, no. 3, pp. 419–436, 2014.

Ahmed, S., Numerical Analysis for Magnetohydrodynamic Chemically Reacting and Radiating Fluid past a Non-Isothermal Impulsively Started Vertical Surface Adjacent to a Porous Regime, *Ain Shams Eng. J.*, vol. **5**, pp. 923–933, 2014.

Ahmed, S. and Kalita, K., Analytical and Numerical Study for MHD Radiating Flow over an Infinite Vertical Plate Bounded by a Porous Medium in Presence of Chemical Reaction, *J. Appl. Fluid Mech.*, vol. **6**, no. 4, pp. 597–607, 2013.

Ahmed, S., Bég, O.A., and Ghosh, S.K., A Couple Stress Fluid Modeling on Free Convection Oscillatory Hydromagnetic Flow in an Inclined Rotating Channel, *Ain Shams Eng. J.*, vol. **5**, pp. 1249–1265, 2014b.

Ahmed, S., Transient Three Dimensional Flow through a Porous Medium with Transverse Permeability Oscillating with Time, *Emirate J. Eng. Res.*, vol. **13**, pp. 11–17, 2008.

Ahmed, S., Free Convective Transient Three-Dimensional Flow through a Porous Medium Oscillating with Time in Presence of Periodic Suction Velocity, *Int. J. Appl. Math. Mech.*, vol. **6**, pp. 1–16, 2010.

Ahmed, S., Induced Magnetic Field with Radiating Fluid over a Porous Vertical Plate: Analytical Study, *J. Naval Archit. Mar. Eng.*, vol. **7**, pp. 83–94, 2010.

Ahmed, S., Mathematical Model of Induced Magnetic Field, with Viscous/Magnetic Dissipation Bounded by a Porous Vertical Plate in Presence of Radiation, *Int. J. Appl. Math. Mech.*, vol. **8**, no. 1, pp. 86–104, 2012.

Ahmed, S. and Kalita, K., A Sinusoidal Fluid Injection/Suction on MHD Three-Dimensional Couette Flow through a Porous Medium in the Presence of Thermal Radiation, *J. Energy Heat Mass Transf.*, vol. **35**, pp. 41–67, 2012a.

Ahmed, S. and Kalita, K., Magnetohydrodynamic Transient Flow through a Porous Medium Bounded by a Hot Vertical Plate in Presence of Radiation: A Theoretical Analysis, *J. Eng. Phys. Thermophys.*, vol. **86**, no. 1, pp. 31–39, 2012b.

Ahmed, S., Batin, A., and Chamkha, A.J., Finite Difference Approach in Porous Media Transport Modeling for Magnetohydrodynamic Unsteady Flow over a Vertical Plate: Darcian Model, *Int. J. Numer. Methods Heat Fluid Flow*, vol. **24**, no. 5, pp. 1204–1223, 2014a.

Ahmed, S., Batin, A., and Chamkha, A.J., Numerical/Laplace Transform Analysis for MHD Radiating Heat/Mass Transport in a Darcian Porous Regime Bounded by an Oscillating Vertical Surface, *Alex. Eng. J.*, vol. **54**, pp. 45–54, 2015.

Ellahi, R., Shivanian, E., Abbasbandy, S., Rahman, S.U., and Hayat, T., Analysis of Steady Flows in Viscous Fluid with Heat Transfer and Slip Effects, *Int. J. Heat Mass Transf.*, vol. **55**, nos. 23-24, pp. 6384–6390, 2012. DOI: 10.1016/j.ijheatmasstransfer.2012.06.026

Ellahi, R. and Hameed, M., Numerical Analysis of Steady Non-Newtonian Flows with Heat Transfer Analysis, MHD and Nonlinear Slip Effects, *Int. J. Numer. Methods Heat Fluid Flow*, vol. **22**, no. 1, pp. 24–38, 2012.

Hayat, T., Qayyum, S., Khan, M.I., and Alsaedi, A., Entropy Generation in Magnetohydrodynamic Radiative Flow due to Rotating Disk in Presence of Viscous Dissipation and Joule Heating, *Phys. Fluids*, vol. **30**, p. 017101, 2018.

Hayat, T., Khan, M.W.A., Alsaedi, A., and Khan, M.I., Squeezing Flow of Second Grade Liquid Subject to Non-Fourier Heat Flux and Heat Generation/Absorption, *Colloid Polym. Sci.*, vol. **295**, pp. 967–975, 2017a.

Hayat, T., Khan, M.I., Farooq, M., Alsaedi, A., and Yasmeen, T., Impact of Cattaneo–Christov Heat Flux Model in Flow of Variable Thermal Conductivity Fluid over a Variable Thicked Surface, *Int. J. Heat Mass Transf.*, vol. **99**, pp. 702–710, 2016.

Hayat, T., Khan, M.I., Waqas, M., and Alsaedi, A., On Cattaneo–Christov Heat Flux in the Flow of Variable Thermal Conductivity Eyring–Powell Fluid, *Results Phys.*, vol. **7**, pp. 446–450, 2017b.

Hayat, T., Waqas, M., Khan, M.I., Alsaedi, A., and Shehzad, S.A., Magnetohydrodynamic Flow of Burgers Fluid with Heat Source and Power Law Heat Flux, *Chin. J. Phys.*, vol. **55**, pp. 318–330, 2017c.

Hayat, T., Khan, M.I., Waqas, M., and Alsaedi, A., Newtonian Heating Effect in Nanofluid Flow by a Permeable Cylinder, *Results Phys.*, vol. **7**, pp. 256–262, 2017d.

Hossain, M.A., and Takhar, H.S., Radiation Effect on Mixed Convection along a Vertical Plate with Uniform Surface Temperature, *Heat Mass Transf.*, vol. **31**, pp. 243–248, 1996.

Ibrahim, F.S., Elaiw, A.M., and Bakr, A.A., Effect of the Chemical Reaction and Radiation Absorption on the Unsteady MHD Free Convection Flow past a Semi Infinite Vertical Permeable Moving Plate with Heat Source and Suction, *Commun. Nonlinear Sci. Numer. Simul.*, vol. **13**, pp. 1056–1066, 2008.

Jaiswal, B.S. and Soundalgekar, V.M., Oscillating Plate Temperature Effects on a Flow past an Infinite Vertical Porous Late with Constant Suction and Embedded in a Porous Medium, *Heat Mass Transf.*, vol. **37**, pp. 125–131, 2001.

Khan, M.I., Waqas, M., Alsaedi, A., Hayat, T., and Khan, M.I., Theoretical Investigation of the Doubly Stratified Flow of an Eyring-Powell Nanomaterial via Heat Generation/Absorption, *Eur. Phys. J. Plus*, vol. **132**, p. 489, 2017a.

Khan, M.I., Waqas, M., Hayat, T., and Alsaedi, A., A Comparative Study of Casson Fluid with Homogeneous-Heterogeneous

Reactions, *Colloids Interface Sci.*, vol. **498**, pp. 85–90, 2017b.

Kim, Y.J., Heat and Mass Transfer in MHD Micropolar Flow over a Vertical Moving Porous Plate in a Porous Medium, *Transp. Porous Media*, vol. **56**, no. 1, pp. 17–37, 2004.

Kumar, A.G.V. and Verma, S.V.K., Thermal Radiation and Mass Transfer Effects on MHD Flow past a Vertical Oscillating Plate with Variable Temperature Effects Variable Mass Diffusion, *Int. J. Eng.*, vol. **3**, pp. 493–499, 2011.

Kumar, S., A New Fractional Modeling Arising in Engineering Sciences and Its Analytical Approximate Solution, *Alex. Eng. J.*, vol. **52**, no. 4, pp. 813–819, 2013.

Mahmoud, A.A. and Chamkha, A.J., Non-Similar Solutions for Heat and Mass Transfer from a Surface Embedded in a Porous Medium for Two Prescribed Thermal and Solutal Boundary Conditions, *Int. J. Chem. Reactor Eng.*, vol. **8**, pp. 1–24, 2010.

Pal, D. and Talukdar, B., Influence of Fluctuating Thermal and Mass Diffusion on Unsteady MHD Buoyancy-Driven Convection past a Vertical Surface with Chemical Reaction and Soret Effects, *Commun. Nonlinear Sci. Numer. Simul.*, vol. **17**, pp. 1597–1614, 2012.

Raptis, A. and Kafoussias, N.G., Magnetohydrodynamic Free Convection Flow and Mass Transfer through Porous Medium Bounded by an Infinite Vertical Porous Plate with Constant Heat Flux, *Can. J. Phys.*, vol. **60**, no. 12, pp. 1725–1729, 1982.

Raptis, A. and Perdikis, C., Unsteady Flow through a Highly Porous Medium in the Presence of Radiation, *Transp. Porous Media*, vol. **57**, pp. 171–179, 2004.

Raptis, A. and Perdikis, C., Radiation and Free Convection Flow past a Moving Plate, *Int. J. Appl. Mech. Eng.*, vol. **4**, pp. 817–821, 1999.

Sattar, M.A., Unsteady Hydromagnetic Free Convection Flow with Hall Current Mass Transfer and Variable Suction through a Porous Medium near an Infinite Vertical Porous Plate with Constant Heat Flux, *Int. J. Energy Res.*, vol. **17**, pp. 1–5, 1993.

Soundalgekar, V.M. and Takhar, H.S., Radiation Effects on Free Convection Flow past a Semi-Infinite Vertical Plate, *Model. Meas. Control B*, vol. **51**, pp. 31–40, 1993.

Swarnalathamma, B.V. and Veera Krishna, M., Peristaltic Hemodynamic Flow of Couple Stress Fluid through a Porous Medium under the Influence of Magnetic Field with Slip Effect, *AIP Conf. Proc.*, vol. **1728**, p. 020603, 2016.

Veera Krishna, M., Hall and Ion Slip Impacts on Unsteady MHD Free Convective Rotating Flow of Jeffreys Fluid with Ramped Wall Temperature, *Int. Commun. Heat Mass Transf.*, vol. **119**, p. 104927, 2020.

Veera Krishna, M. and Chamkha, A.J., Hall Effects on Unsteady MHD Flow of Second Grade Fluid through Porous Medium with Ramped Wall Temperature and Ramped Surface Concentration, *Phys. Fluids*, vol. **30**, p. 023106, 2018.

Veera Krishna, M. and Chamkha, A.J., Hall Effects on MHD Squeezing Flow of a Water based Nano Fluid between Two Parallel Disks, *J. Porous Media*, vol. **22**, no. 2, pp. 209–223, 2019a.

Veera Krishna, M. and Chamkha, A.J., Hall and Ion Slip Effects on MHD Rotating Boundary Layer Flow of Nanofluid past an Infinite Vertical Plate Embedded in a Porous Medium, *Results Phys.*, vol. **15**, p. 102652, 2019b.

Veera Krishna, M. and Chamkha, A.J., Hall and Ion Slip Effects on Unsteady MHD Convective Rotating Flow of Nanofluids—Application in Biomedical Engineering, *J. Egypt. Math. Soc.*, vol. **28**, no. 1, pp. 1–14, 2020a.

Veera Krishna, M. and Chamkha, A.J., Hall and Ion Slip Effects on MHD Rotating Flow of Elastico-Viscous Fluid through Porous Medium, *Int. Commun. Heat Mass Transf.*, vol. **113**, p. 104494, 2020b.

Veera Krishna, M. and Gangadhar Reddy, M., MHD Free Convective Rotating Flow of Visco-Elastic Fluid past an Infinite Vertical Oscillating Porous Plate with Chemical Reaction, *IOP Conf. Series: Mater. Sci. Eng.*, vol. **149**, p. 012217, 2016.

Veera Krishna, M. and Gangadhar Reddy, M., MHD Free Convective Boundary Layer Flow through Porous Medium past a Moving Vertical Plate with Heat Source and Chemical Reaction, *Mater. Today: Proc.*, vol. **5**, pp. 91–98, 2018.

Veera Krishna, M. and Jyothi, K., Hall Effects on MHD Rotating Flow of a Visco-Elastic Fluid through a Porous Medium over an Infinite Oscillating Porous Plate with Heat Source and Chemical Reaction, *Mater. Today: Proc.*, vol. **5**, pp. 367–380, 2018.

Veera Krishna, M. and Subba Reddy, G., Unsteady MHD Convective Flow of Second Grade Fluid through a Porous Medium in a Rotating Parallel Plate Channel with Temperature Dependent Source, *IOP Conf. Series: Materials Sci. Eng.*, vol. **149**, p. 012216, 2016.

Veera Krishna, M. and Subba Reddy, G., MHD Forced Convective Flow of Non-Newtonian Fluid through Stumpy Permeable Porous Medium, *Mater. Today: Proc.*, vol. **5**, pp. 175–183, 2018a.

Veera Krishna, M. and Swarnalathamma, B.V., Convective Heat and Mass Transfer on MHD Peristaltic Flow of Williamson Fluid

with the Effect of Inclined Magnetic Field, *AIP Conf. Proc.*, vol. **1728**, p. 020461, 2016.

Veera Krishna, M., Swarnalathamma, B.V., and Prakash, J., Heat and Mass Transfer on Unsteady MHD Oscillatory Flow of Blood through Porous Arteriole, Applications of Fluid Dynamics, *Lect. Notes Mech. Eng.*, vol. **XXII**, pp. 207–224, 2018a.

Veera Krishna, M., Subba Reddy, G., and Chamkha, A.J., Hall Effects on Unsteady MHD Oscillatory Free Convective Flow of Second Grade Fluid through Porous Medium between Two Vertical Plates, *Phys. Fluids*, vol. **30**, p. 023106, 2018b.

Veera Krishna, M., Gangadhar Reddy, M., and Chamkha, A.J., Heat and Mass Transfer on MHD Free Convective Flow over an Infinite Nonconducting Vertical Flat Porous Plate, *Int. J. Fluid Mech. Res.*, vol. **45**, no. 5, pp. 1–25, 2018c.

Veera Krishna, M., Jyothi, K., and Chamkha, A.J., Heat and Mass Transfer on Unsteady, Magnetohydrodynamic, Oscillatory Flow of Second-Grade Fluid through a Porous Medium between Two Vertical Plates, under the Influence of Fluctuating Heat Source/Sink and Chemical Reaction, *Int. J. Fluid Mech. Res.*, vol. **45**, no. 5, pp. 1–19, 2018d.

Veera Krishna, M., Ameer Ahamad, N., and Chamkha, A.J., Hall and Ion Slip Effects on Unsteady MHD Free Convective Rotating Flow through a Saturated Porous Medium over an Exponential Accelerated Plate, *Alexandria Eng. J.*, vol. **59**, pp. 565–577, 2020a.

Veera Krishna, M., Sravanthi, C.S., and Gorla, R.S.R., Hall and Ion Slip Effects on MHD Rotating Flow of Ciliary Propulsion of Microscopic Organism through Porous Media, *Int. Commun. Heat Mass Transf.*, vol. **112**, p. 104500, 2020b.

Veera Krishna, M., Jyothi, K., and Chamkha, A.J., Heat and Mass Transfer on MHD Flow of Second-Grade Fluid through Porous Medium over a Semi-Infinite Vertical Stretching Sheet, *J. Porous Media*, vol. **23**, no. 8, pp. 751–765, 2020c.

Waqas, M., Khan, M.I., Hayat, T., Alsaedi, A., and Imran Khan, M., On Cattaneo–Christov Double Diffusion Impact for Temperature-Dependent Conductivity of Powell–Eyring Liquid, *Chin. J. Phys.*, vol. **55**, pp. 729–737, 2017.

Zeidan, D., Alnaief, M., Ziad Saghir, M., and Touma, R., Simulations on Porous Media with Nanofluids–Initial Study, *AIP Conf. Proc.*, vol. **1738**, p. 030006, 2016.

Zueco, J., Ahmed, S., and López-Ochoa, L.M., Magneto-Micropolar Flow over a Stretching Surface Embedded in a Darcian Porous Medium by Numerical Network Method, *Arab. J. Sci. Eng.*, vol. **39**, no. 6, pp. 5141–5151, 2014.

Zueco, J., Unsteady Free Convection-Radiation Flow over a Vertical Wall Embedded in a Porous Medium, *Commun. Numer. Methods Eng.*, vol. **24**, pp. 1093–1105, 2008.